W.-L. Huang, S.-S. Li, Z. Ren, and C. T.-C. Nguyen, "UHF nickel micromechanical spoke-supported ring resonators," *Dig. of Tech. Papers*, the 14th Int. Conf. on Solid-State Sensors & Actuators (Transducers'07), Lyon, France, June 11-14, 2007, pp. 323-326.

UHF NICKEL MICROMECHANICAL SPOKE-SUPPORTED RING RESONATORS

Wen-Lung Huang[1], Sheng-Shian Li[1], Zeying Ren[1], and Clark T.-C. Nguyen[2]

[1]University of Michigan
Ann Arbor, Michigan, USA 48109-2122
[2]University of California at Berkeley
Berkeley, California, USA 94720-1770

Abstract: A micromechanical vibrating spoke-supported ring resonator fabricated in a low deposition temperature nickel metal material has been demonstrated in two vibration modes spanning frequencies from HF (18 MHz) to UHF (425.7 MHz) with *Q*'s as high as 6,405 and 2,467, respectively. The use of an anchor isolating spoke-supported ring geometry along with notched support attachments between the ring structure and supporting beams contributes to demonstration of the highest reported vibrating frequency to date for any *macro* or *micro*-scale metal resonator, making this the first metal micromechanical resonator suitable for RF applications. Because the nickel structural material is deposited at 50°C, the fabrication process for this resonator is quite amenable to post-processing over finished foundry CMOS wafers, even ones with gate lengths below 65 nm slated to use advanced low-k (but low melting point from 300-400°C) dielectric material around their metals. This makes nickel structural material an attractive choice for low cost post-transistor single-chip integration of high *Q* vibrating passives with transistor circuits for wireless applications.

Keywords: material properties, micromechanical resonators, nickel, quality factor, RF MEMS.

1. INTRODUCTION

The history of efforts to employ nickel as a micromechanical resonator structural material is peppered with encumbering issues, such as insufficient frequency [1], where frequencies larger than 1 MHz were non-existent before 2006; insufficient *Q*'s [1] of only 2,400 until 1999, when *Q*'s >10,000 were finally attained, but at sub-100 kHz [2]; and excessive aging and drift [1][2]. The localized annealing work of [3] did much to mitigate the *Q* and drift issues at sub-100kHz frequencies, but no nickel resonator over 1 MHz could be demonstrated with a *Q* >1,000 sufficient for communications applications until very recently, when the 2006 work of [4] demonstrated a 60-MHz wine-glass disk resonator with a *Q* =54,507. But 60 MHz is still insufficient for RF applications, which require frequencies in the 100's of MHz or GHz range.

The present work extends for the first time the frequency range of nickel micromechanical resonators to the needed RF frequency range while still retaining a *Q* high enough (i.e., >1,000) for RF filtering and oscillator applications. In this work, a MEMS-based vibrating ring resonator fabricated in a low temperature nickel metal material and using a 33-nm nitride dielectric capacitive transducer has been demonstrated at a frequency of 425.7 MHz with *Q*'s as high as 2,467, which is the highest reported to date for any *micro*-scale metal resonator in the UHF range. Because the highest fabrication temperature in this process is 380°C, and there is a path to an even lower temperature ceiling (e.g., room tempera-

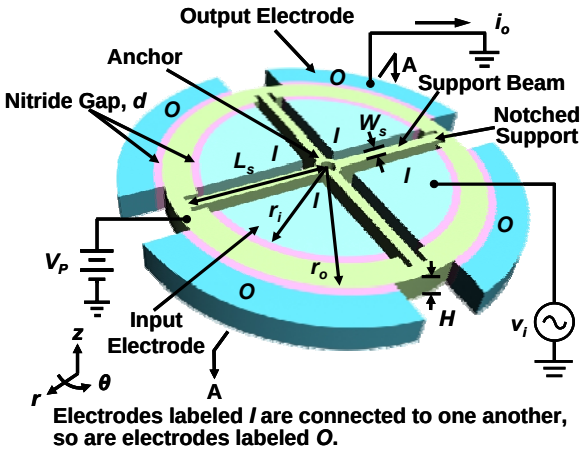

Fig. 1: Perspective view schematic of a micromechanical spoke-supported ring resonator, identifying key dimensions and showing a typical two-port bias and excitation configuration.

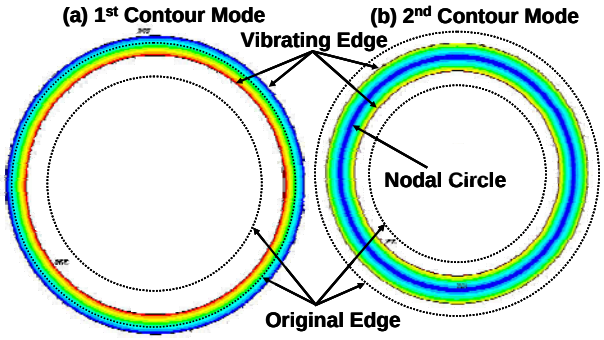

Fig. 2: Finite element simulated (a) 1st contour mode (symmetric mode) and (b) 2nd contour mode shape (anti-symmetric mode) for the nickel ring resonator of Fig. 1.

ture), the fabrication process for this resonator is quite amenable to post-processing over finished foundry CMOS wafers, even those with gate lengths below 65 nm slated to use advanced low-k (but low melting point from 300-400°C) dielectric material around their metals [5].

2. DEVICE OPERATION AND DESIGN

Fig. 1 presents a perspective view schematic of the ring resonator design used in this work, identifying key dimensions and indicating a two-port bias and excitation scheme. The device is similar to that of [6] and comprises a 3μm-thick nickel ring resonator suspended 400 nm above a ground plane by four spokes centrally anchored to an underlying ground plane. Eight electrodes are placed at four quadrants overlapping the inside and outside of the ring so as to specifically excite the ring into one of the two contour mode shapes, shown in Fig. 2.

To operate this device in its two-port configuration shown in Fig. 1, a dc-bias voltage V_P is applied to the ring structure and an ac signal v_i to its inner electrodes, creating a time varying electrostatic force acting on the ring. When the input signal acts at the anti-symmetric resonance frequency of the device, the effect of that force is multiplied by the Q factor of the resonator, resulting in expansion and contraction of the ring around its CAD-defined width along its inner and outer perimeters, as shown in the anti-symmetric mode shape of Fig. 2(b). This vibrating motion results in a time-varying dc-biased capacitor between the ring and the output electrodes generating a combined output current i_o at the vibrational resonance frequency of the ring, which is governed primarily by its material properties and its width [6].

From [7], the presence of a solid dielectric-filled gap between a lateral resonator and its electrodes does not necessarily constitute a dominating loss mechanism that dictates Q. The wine-glass device of [7] in fact achieved Q's in excess of 35,000, despite its use of solid gaps. Thus, for the present ring resonator design, one might initially assume that losses contributed by its solid-gap resonator-to-electrode interface are important only if the Q of the overall resonator is on the order of 35,000. From [6], this is not the case even for UHF rings constructed of polysilicon.

Thus, even with solid-gap capacitive transducers, given that anchor losses generally dominate the Q's of previous air-gap UHF resonators, the use of lossless anchor design for the present nickel ring resonator is still important and beneficial. The design of Fig. 1 thus features the isolating spoke-support design first detailed in [6], where the spokes are dimensioned to correspond to a quarter-wavelength at the ring's resonance frequency, and where notches are used to better access the extensional contour mode nodal circle, like that of Fig. 2(b).

3. EXPERIMENTAL RESULTS

The ring resonators in this work were fabricated via a lateral solid-gap transducer nickel plating process, similar to that reported in [4] for previous nickel wine-glass mode disk resonators, except this time using SPR220-3.0 as the structure plating mold, instead of AZ9260, in an effort to achieve the 1.5μm support beam features needed to attain Q's in the thousands. In this process, the temperature during nickel electroplating is 50°C, and the highest temperature step is 380°C for the PECVD silicon nitride gap material, which can be lowered via use of atomic layer deposition (ALD), or some other lower temperature dielectric deposition process. Fig. 3 presents the final cross-section for the nickel ring resonator constructed in this process, taken along the AA plane of Fig. 1. Fig. 4 presents the global-view SEM of the ring resonator and a zoom-in SEM on one of its notched support attachment locations.

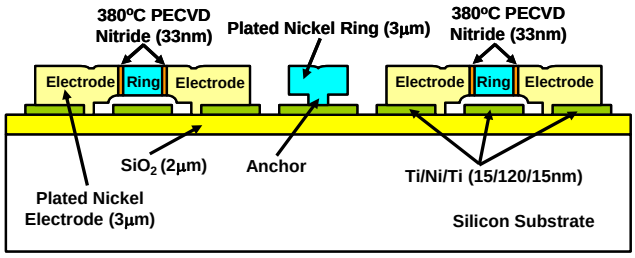

Fig. 3: Final cross-section for the nickel ring resonator constructed in this process.

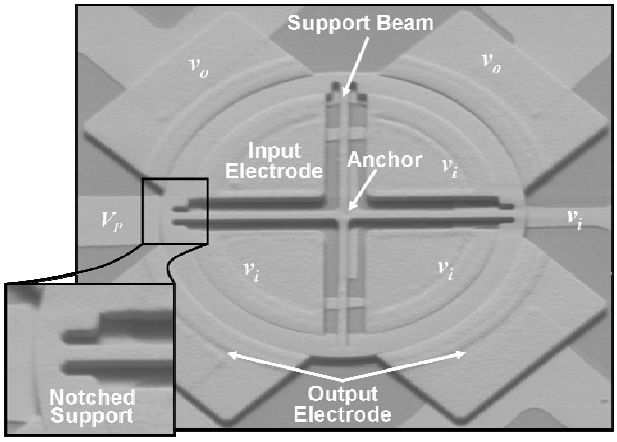

Fig. 4: Global-view SEM of the ring resonator and a zoom-in SEM on one of its notched support attachment locations.

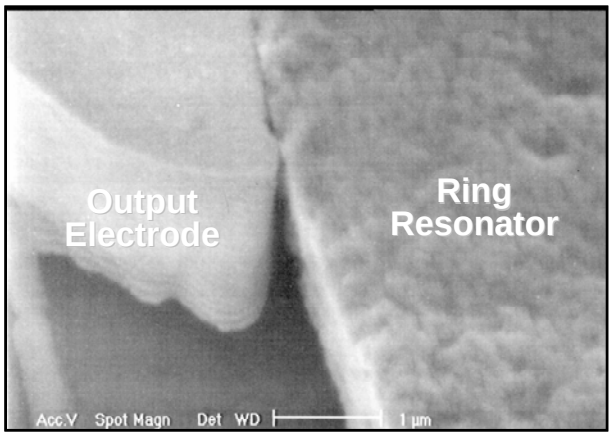

Fig. 5: Gap-zoomed SEM of the incomplete electrode-to resonator overlap.

Despite the use of a slower electroplating rate during electrode formation, the electrodes for the ring devices of this work still exhibited the same undercutting near the ring sidewalls seen in [4], and shown in Fig. 5. The resultant incomplete electrode-to-resonator overlap raised the motional

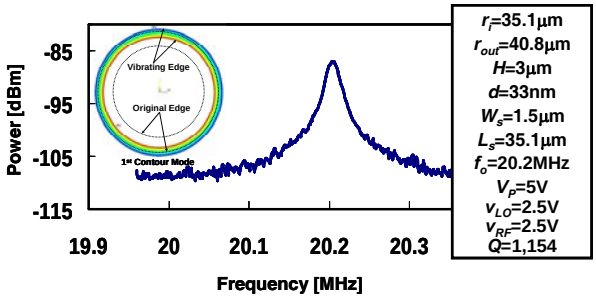

Fig. 6: Frequency characteristic of a fabricated nickel ring resonator with direct support attachments operated at its first radial contour mode centered at 20.2 MHz, measured via a mixing measurement technique.

impedances of the rings to several hundred kΩ's, which made direct two-port measurement of the devices quite difficult, since the expected motional current ends up being smaller than feedthrough currents at UHF. To circumvent this problem, a mixing measurement technique [8] was used to test the nickel rings. Briefly, mixing suppresses the impact of feedthrough currents by moving them away from motional currents in the frequency domain.

Fig. 6 presents the measured frequency characteristic for the first radial contour mode of a ring resonator with direct-support attachments (as opposed to notched support), centered at 20.2 MHz with a measured Q of 1,154. Next, a ring resonator with notched support attachment was tested. Fig. 7 presents the measured frequency characteristic for its first radial contour mode, showing a much higher Q of 6,405 at 18 MHz, verifying that careful support design is still beneficial even when solid-gap capacitive transducers are utilized.

Finally, Fig. 8 presents the measured frequency characteristic of this ring's second radial contour mode, vibrating at 425.7 MHz with a Q of 2,467, which is on par with some polysilicon ring resonators [9], and which verifies that nickel could be every bit as good as polysilicon in attaining high Q at high frequency.

4. CONCLUSIONS

In achieving a Q of 2,467 at 425.7 MHz, the nickel spoke-supported micromechanical ring resonator of this work attains the highest fre-

Table 1: UHF Micromechanical Resonator Material Comparison

Material	Acoustic Velocity (m/s)	Deposition Temperature (^{o}C)	Electrical Conductivity (10^{7}/Ωm)	*1 GHz Ring Dimensions* r_i ; r_{out} (μm)
Polysilicon	8,024	588	0.001	35.1 ; 39.2
Polydiamond	18,076	800	0.001	35.1 ; 44.4
Silicon Carbide	11,500	800	0.00083	35.1 ; 41
$PolySi_{0.35}Ge_{0.65}$	5,840	450	0.005	35.1 ; 38.1
Nickel	4,678	50	1.43	35.1 ; 37.5

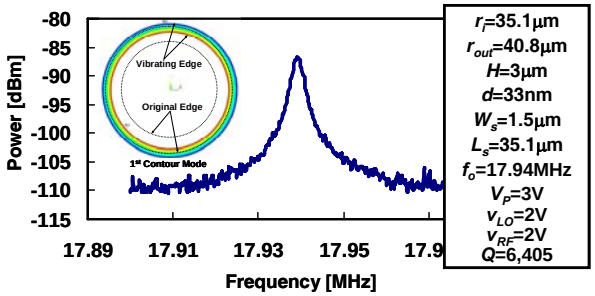

Fig. 7: Frequency characteristic of a fabricated nickel ring resonator with notched support attachments operated at its first radial contour mode centered at 18 MHz, measured via a mixing measurement technique.

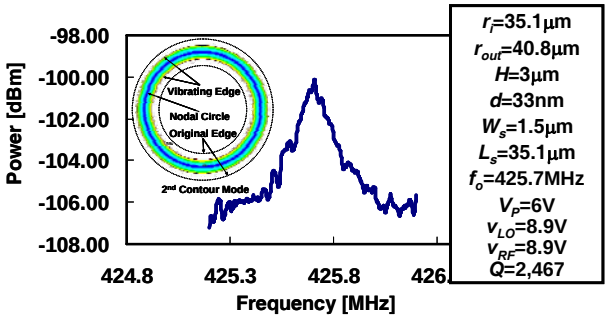

Fig. 8: Frequency characteristic of a fabricated nickel ring resonator with notched support attachments operated at its second radial contour mode centered at 425.7 MHz, measured via a mixing measurement technique

quency reported to date for any *micro-scale* metal resonator device. This achievement, however, begs the question: How does nickel stack up against other high frequency resonator materials?

Table 1 compares the material properties of nickel with other popular resonator materials, showing that although nickel possesses the lowest deposition temperature and highest electrical conductivity, its acoustic velocity is substantially lower than that of the others. However, the ultimate difference in actual dimensional design turns out not so large. As shown in Table 1, for the case of contour mode ring resonators operated at their 2nd mode, the outer radius r_{out} dimensions of a ring with inner radius r_i = 35.1 μm vibrating at 1 GHz are 37.5 and 39.2 μm for nickel and polysilicon, respectively. Although the required dimensions for nickel are smaller, they are still quite manufacturable.

Acknowledgment. This work was supported by an NSF ERC in Wireless Integrated Microsystems.

References.

[1] M. W. Putty, et al., "A micromachined …," *Hilton Head'94*, pp. 213-220.

[2] W.-T. Hsu, et al., "In situ localized …," *Transducers'99*, pp. 932-935.

[3] W.-T. Hsu, et al., "Geometric stress …," *IEEE Ultras. Symp.'98*, pp. 945-948.

[4] W.-L. Huang, et al., "Nickel vibrating …," *IEEE FCS'06*, pp. 839-847.

[5] G. Maier, "The search …," *IEEE Electrical Insulation Magazine*, vol. 20, no. 2, pp. 6-17, Dec. 2004.

[6] S.-S. Li, et al., "Micromechanical "hollow-disk" …," *MEMS'04*, pp. 821-824.

[7] Y.-W. Lin, "Vibrating Micromechanical …," *IEEE FCS'05*, pp. 839-847.

[8] J. Wang, et al., "1.156-GHz self-aligned …," *IEEE Trans. UFFC*, vol. 51, no. 12, pp. 1607-1628, Dec. 2004.

[9] Y. Xie, et al., "UHF micromechanical …," *IEDM'03*, pp. 953-956.